Project), edited by A. Erdélyi (McGraw-Hill, New York, 1953), Vol. 2, p. 116, Eq. (15).
[9]*Higher Transcendental Functions* (Bateman Manuscript Project), edited by A. Erdélyi (McGraw-Hill, New York, 1953), Vol. 2, p. 108, Eqs. (2) and (5).
[10]G. Höhler, H. Schaite, and P. Sonderegger, Phys. Letters 20, 79 (1966).
[11]V. Singh, Phys. Rev. 129, 1889 (1963).
[12]R. Phillips and W. Rarita, Phys. Rev. 139, B1336 (1965).
[13]The exact value of ρ is not critical and other choices are certainly possible, but to keep the number of parameters to be fit by numerical methods down to a minimum, we will assume this to be the correct one.
[14]V. S. Barashenkov, *Interaction Cross Sections of Elementary Particles* (Israel Program of Scientific Translations, Jerusalem, 1968).
[15]T. Gadjicar, R. Logan, and T. Moffat, Phys. Rev. 170, 1599 (1968).
[16]See, for example, R. C. Arnold and M. L. Blackmon, Phys. Rev. 175, 2082 (1968); M. Ross, F. Henyey, and G. Kane, Nucl. Phys. B23, 269 (1970).
[17]Whenever possible, we try to get approximate solutions at special points rather than attempting general optimizations (i.e., least squares, etc.), the significance of which is not always clear when dealing with a new model.
[18]W. Frazer and J. Fulco, Phys. Rev. 117, 1603 (1960).
[19]See Singh (Ref. 11), and for a more general treatment, A. H. Mueller and T. L. Trueman, Phys. Rev. 160, 1296 (1967).
[20]See R. Omnes, in *Strong Interactions and High Energy Physics*, edited by R. G. Moorhouse (Plenum, New York, 1963).
[21]A recent compilation of data on pion-nucleon scattering containing a wealth of references is G. Giacomelli, P. Pini, and S. Stagni, CERN/HERA Report No. 69-1 (unpublished).
[22]R. J. Esterling, N. E. Booth, G. Conforto, J. Parry, J. Scheid, and A. Yokosawa, in *Proceedings of the Fourteenth International Conference on High Energy Physics, Vienna, 1968*, edited by J. Prentki and J. Steinberger (CERN, Geneva, 1968).
[23]The factor α_P is really not necessary since in the range considered, α_P is always close to unity.
[24]We are grateful to Professor M. T. Parkinson for making his optimizing subroutines available to us and for instructing us in their use.
[25]C. B. Chiu, S. Y. Chu, and L. L. Wang, Phys. Rev. 161, 1563 (1967).

PHYSICAL REVIEW D VOLUME 6, NUMBER 1 1 JULY 1972

ϕ^3 Analyticity and Finite-Energy Sum Rule for Inclusive Reactions

A. I. Sanda
National Accelerator Laboratory, Batavia, Illinois 60510
(Received 22 December 1971)

Using ϕ^3 theory as a model, the analytic structure of the six-point function is investigated. Specifically studied is the kinematical region appropriate to the single-particle inclusive reaction where the missing mass is much less than the incident energy. With some idea about the analyticity, a finite-energy sum rule is derived. This sum rule can be used to study the concept of generalized duality. The most striking feature of the sum rule is a possibility that the "triple-Regge vertex function" can be calculated by the data on the inclusive reaction with relatively low missing mass, i.e., the resonance-production region.

I. INTRODUCTION

It has been conjectured that the cross section for

$$a+b\to c+\text{anything} \tag{1}$$

is related to the absorptive part of a scattering amplitude for

$$a+b+\bar{c}\to a+b+\bar{c} \tag{2}$$

when the amplitude is analytically continued to the proper kinematical region.[1] Then various asymptotic behaviors of (1) can be obtained from that of (2). It is assumed that the asymptotic behaviors of (2) can be obtained by the O(2, 1) expansion.[2] Subsequently, it has been verified in the context of field theory that the amplitude for reaction (2), when continued analytically, indeed has an absorptive part which is proportional to the cross section for reaction (1).[3]

We see the analogy between the four-point function and the six-point function developing. The inclusive cross section and the six-point function satisfy a relationship similar to that between the total cross section and the four-point function. The O(2, 1) expansion in the six-point function corresponds to the Regge expansion in the four-point function. We therefore see that the machinery developed for the four-point function (forward-dispersion relations, finite-energy sum rules, etc.)

may be perhaps applicable to the six-point function. What follows is the first attempt along this line.

In order to start the program, we must first get some idea about analyticity. No doubt the problem of analyticity and crossing for the six-point function will be complicated. At present we can gain insight only by investigating a reliable model. For this purpose, we will use ϕ^3 theory as our guide.

The kinematical variables for our problem are

$$s=(p_a+p_b)^2, \qquad p_a^2=m^2,$$
$$t=(p_a-q)^2, \qquad p_b^2=m^2,$$
$$M^2=(p_a+p_b-q)^2, \qquad q^2=\mu^2,$$

where the momenta are defined by Fig. 1.

The result of our analysis indicates that the analyticity on the M^2 plane for fixed $t\leq 0$ and large s and s/M^2 is directly related to the analyticity in the mass variable of an ordinary Regge residue function. Given the possibility that there might be some complex branch point on the M^2 plane in addition to the singularity obtained from unitarity, we must be cautious in applying analytic-function theory to the scattering amplitude. We will, however, assume, for the time being, that such complex branch points are absent. This assumed analyticity, together with the idea of triple-Regge dominance, yields a sum rule which corresponds to the finite-energy sum rule for the four-point function.

In Sec. II we discuss the optical theorem for the six-point function. In Sec. III we consider possibilities for complex cuts and state a theorem on the analyticity of the relevant Feynman diagram. In Sec. IV we prove the theorem. This section can be skipped without loss of continuity. In Sec. V we derive a finite-energy sum rule. In Sec. VI we present sum rules which require additional assumptions about fixed poles, etc.

II. GENERALIZED OPTICAL THEOREM

The cross section for reaction (1) can be written as

$$\frac{d\sigma}{dt\,dM^2}=\frac{m^2}{(2\pi)^2 s^2}A(s,t,M^2),$$

$$A(s,t,M^2)=\lim_{q^2\to\mu^2}\frac{E_aE_b}{m^2}\int d^4x\,e^{-iq\cdot x}(q^2-\mu^2)^2\langle p_ap_b\text{out}|\phi_c^\dagger(x)\phi_c(0)|p_ap_b\text{out}\rangle,$$

where $\phi_c(x)$ is the field operator for particle c. Let T be the amplitude for the process shown in Fig. 2:

$$T=\lim_{q^2\to\mu^2;q'^2\to\mu^2}\frac{E_aE_b}{m^2}\,i\int d^4x\,e^{-iq\cdot x}(q^2-\mu^2)(q'^2-\mu^2)\langle p_ap_b\text{out}|T(\phi_c^\dagger(x)\phi_c(0))|p_ap_b\,\text{in}\rangle. \tag{3}$$

T is a function of 25 Lorentz scalars that can be constructed out of the 6 four-vectors and thus has singularities for 25 different channels.[4] It has been shown that in the forward limit when s and t are fixed, $s>s$-channel threshold, $t<0$, the absorptive part of T in M^2 is proportional to A. We would like to sketch the reasoning behind the above statement. Let us first define what we mean by forward limit. Since the limit is used to relate the cross section to the absorptive part of T, all the four-vectors must approach a real limit. That is, $\lim p_i=\lim p_i'=$ real four-vector, $\lim q=\lim q'=$ real four-vector. But it is important to keep in mind that the direction and the rate at which these four-vectors approach the limit is not specified. For example, in the special frame in which $\vec{p}_a=0$, we can have

$$p_a=(m,0,0,0), \qquad p_a'=(m,0,0,0),$$
$$p_b=(E+i\epsilon_b,0,0,p_z), \qquad p_b'=(E-i\epsilon_b',0,0,p_z'),$$
$$q=(q_0+i\epsilon_c,q_x,0,q_z), \qquad q'=(q_0+i\epsilon_c',q_x,0,q_z).$$

In the forward limit, all ϵ's approach zero, but it is our choice as to how they go to zero. In what follows, we make the distinction between primed and unprimed variables only if it is important to keep track of

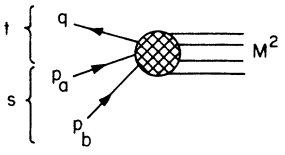

FIG. 1. Diagram for an inclusive process.

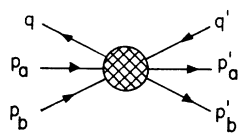

FIG. 2. Diagram for a six-point function.

$i\epsilon$'s. In the forward limit when s and t are fixed and $s > s$-channel threshold, $t < 0$, only those variables that are linearly related to $p_b \cdot q$, $p_b \cdot q'$, or $p_b' \cdot q$ can vary. They are

$$\begin{aligned}
&M^2 = (p_a + p_b - q)^2, \quad M_1^2 = (p_a - p_b' - q)^2 = 2t + 2m^2 - M^2,\\
&M_2^2 = (p_a + p_b + q')^2 = s + s' + 2\mu^2 - M^2, \quad M_3^2 = (-p_a' + p_b - q)^2 = 6m^2 + 2\mu^2 - s - s' - 2t + M^2,\\
&\chi_4 = (p_b - q)^2 = 2m^2 + \mu^2 + M^2 - s - t, \quad \chi_5 = (p_b' - q')^2 = 2m^2 + \mu^2 + M^2 - s' - t,\\
&\chi_7 = (p_b + q')^2 = s' + \mu^2 - M^2 + t, \quad \chi_8 = (p_b' + q)^2 = s + \mu^2 - M^2 + t,
\end{aligned} \tag{4}$$

where we have set $p_a^2 = p_b^2 = m^2$. These channels are shown in Fig. 3. The absorptive part in M^2, when $s = s_0 + i\epsilon_1$, $s' = s_0 + i\epsilon_2$, t real is

$$\begin{aligned}
2i\mathrm{Abs}T = {} & T(s = s_0 + i\epsilon_1, s' = s_0 + i\epsilon_2, t, M^2 = M_0^2 + i\epsilon_3, M_1^2 = 2t + 2m^2 - M_0^2 - i\epsilon_3,\\
& M_2^2 = 2s_0 + 2\mu^2 - M_0^2 + i(\epsilon_1 + \epsilon_2 - \epsilon_3), M_3^2 = 6m^2 + 2\mu^2 - 2s_0 - 2t + M_0^2 + i(-\epsilon_1 - \epsilon_2 + \epsilon_3),\\
& \chi_7 = s_0 + \mu^2 + t - M_0^2 + i(\epsilon_2 - \epsilon_3), \chi_8 = s_0 + \mu^2 + t + i(\epsilon_1 - \epsilon_3),\\
& \chi_4 = -s_0 + M_0^2 + 2m^2 + \mu^2 - t + i(-\epsilon_1 + \epsilon_3), \chi_5 = -s_0 + M_0^2 + 2m^2 + \mu^2 - t + i(\epsilon_2 + \epsilon_3))\\
& - T(s = s_0 + i\epsilon_1, s' = s_0 + i\epsilon_2, M^2 = M_0^2 - i\epsilon_3, M_1^2 = 2t + 2m^2 - M_0^2 + i\epsilon_3,\\
& M_2^2 = 2s_0 + 2\mu^2 - M_0^2 + i(\epsilon_1 + \epsilon_2 + \epsilon_3), M_3^2 = 6m^2 + 2\mu^2 - 2s_0 - 2t + M_0^2 + i(-\epsilon_1 - \epsilon_2 - \epsilon_3),\\
& \chi_7 = s_0 + \mu^2 + t - M_0^2 + i(\epsilon_2 + \epsilon_3), \chi_8 = s_0 + \mu^2 + t + i(\epsilon_1 + \epsilon_3),\\
& \chi_4 = -s_0 + M_0^2 + 2m^2 + \mu^2 - t + i(-\epsilon_1 - \epsilon_3), \chi_5 = -s_0 + M_0^2 + 2m^2 + \mu^2 - t + i(\epsilon_2 - \epsilon_3)).
\end{aligned} \tag{5}$$

Note that if we choose ϵ_1, ϵ_2, ϵ_3 such that $|\epsilon_1| > |\epsilon_3|$, $|\epsilon_2| > |\epsilon_3|$, only the discontinuity in M^2 and M_1^2 contributes to the difference. All other channel variables are evaluated on the same side of their respective cuts. [That is, the small imaginary part of all variables except M^2 and M_1^2, does not change sign between two terms on the right-hand side of Eq. (5), the unitarity equation.]. In other words T has singularities corresponding to each channel associated with the variables listed in footnote 4, but it is possible to isolate a sheet on the M^2 plane which contains only the singularities due to the M^2 and M_1^2 channels. From now on, "M^2 plane" refers to this sheet. The absorptive part of T in M^2 can be evaluated from Eq. (3).

$$\begin{aligned}
\mathrm{Abs}_{M^2} T(s = s_0 + i\epsilon_1, s' = s_0 + i\epsilon_2, t, M^2) &= \lim_{q^2 \to \mu^2} \sum_n \frac{E_a E_b}{m^2} (q^2 - \mu^2)^2 (2\pi)^4 [\, \delta^4(p_a + p_b - q - p_n) \langle p_a p_b \,\mathrm{out}|\phi_c^\dagger(0)|n\rangle\langle n|\phi_c(0)|p_a p_b \,\mathrm{in}\rangle\\
&\quad + \delta^4(p_a - p_b' - q - p_n) \langle p_a p_b \,\mathrm{out}|\phi_c^\dagger(0)|n\rangle\langle n|\phi_c(0)|p_a p_b \,\mathrm{in}\rangle\,].
\end{aligned}$$

Note that the first term on the right-hand side is nonzero only if $p_a + p_b - q = p_n$ and the second term is nonzero only if $p_a - p_b' - q = p_n$. These two regions do not overlap. Consider the region where $p_a + p_b - q = p_n$. We want to show that

$$\mathrm{Abs}_{M^2} T(s = s_0 + i\epsilon_1, s' = s_0 - i\epsilon_1, t, M^2) = A, \tag{6}$$

where

$$A = \lim_{q^2 \to \mu^2} \sum_n \frac{E_a E_b}{m^2} (q^2 - \mu^2)^2 (2\pi)^4 \delta^4(p_a + p_b - q - p_n) \langle p_a p_b \,\mathrm{in}|\phi_c^\dagger(0)|n\rangle\langle n|\phi_c(0)|p_a p_b \,\mathrm{in}\rangle.$$

Of course the distinction between Abs$T$ and A are "in" and "out" states. Let us define an analytic function $F(s, M^2, t)$ such that

$$\lim_{\epsilon_1, \epsilon_3 \to 0} F_n(s_0 + i\epsilon_1, M^2 + i\epsilon_3, t) = \left(\frac{E_a E_b}{m^2}\right)^{1/2} \langle p_a p_b \,\mathrm{out}|\phi_c^\dagger(0)|n\rangle.$$

Then Eq. (6) is proven if we can show that

$$\lim_{\epsilon_1, \epsilon_3 \to 0} F_n(s_0 - i\epsilon_1, M^2 + i\epsilon_3, t) = \left(\frac{E_1 E_2}{m^2}\right)^{1/2} \langle n|\phi(0)|p_a p_b \,\mathrm{in}\rangle^* \tag{7}$$

since the continuation of T from $s' = s_0 + i\epsilon_1$ to $s' = s_0 - i\epsilon_1$ is given by the continuation of F_n from $s' = s_0 + i\epsilon_1$ to $s' = s_0 - i\epsilon_1$. Let $t < 0$ and thus be below the t-channel threshold. By reducing b we obtain[5]

$$\left(\frac{E_a E_b}{m^2}\right)^{1/2}\langle p_a p_b \text{ out}|\phi^\dagger(0)|n\rangle = \lim_{\epsilon_1\to 0;\epsilon_2\to 0} F(s_0+i\epsilon_1, M_0^2+i\epsilon_3, t)$$

$$= \lim_{\epsilon_1\to 0;\epsilon_3\to 0}\lim_{p_b^2\to m_b^2}\int d^3x\, e^{-i\vec{p}_b\cdot\vec{x}}(p_b^2-m^2)\left[\left\langle p_a\left|\phi_b(\vec{x},0)\frac{1}{p_b^0+p_a^0-H-i\epsilon}\,\phi_c^\dagger(0)\right|n\right\rangle\right.$$

$$\left.+\left\langle p_a\left|\phi_c^\dagger(0)\frac{1}{p_n^0-p_b^0-H-i\epsilon}\,\phi_b(\vec{x},0)\right|n\right\rangle\right], \tag{8}$$

where we have performed the x_0 integration by using an integral representation for the θ function. If we evaluate Eq. (8) in the rest frame of a,

$$s = 2(m^2 + mE + im\epsilon_b + iE\epsilon_b),$$

the continuation to the opposite side of the cut in s is equivalent to continuing p_b^0 to the other side of its cut. On the other side of the cut in p_b^0, the sign of $i\epsilon$ changes:

$$F(s_0 - i\epsilon_1, M^2+i\epsilon_3, t) = \lim_{p_b^2\to m^2}\left(\frac{E_a}{m}\right)^{1/2}\int d^3x\, e^{-i\vec{p}_b\cdot\vec{x}}(p_b^2-m^2)\left[\left\langle p_a\left|\phi_b(\vec{x},0)\frac{1}{p_b^0+p_a^0-H+i\epsilon}\,\phi_c^\dagger(0)\right|n\right\rangle\right.$$

$$\left.+\left\langle p_a\left|\phi_c^\dagger(0)\frac{1}{p_n^0-p_b^0-H+i\epsilon}\,\phi_b(\vec{x},0)\right|n\right\rangle\right].$$

If b is reduced in $(E_a E_b/m_a m_b)^{1/2}\langle n|\phi(0)|p_a p_b \text{ in}\rangle$, it is quite easily seen that indeed Eq. (7) holds.

We stress again the most important point: *there is a sheet in the M^2 plane which contains only the M^2- and M_1^2-channel singularities*. If the singularities from the other channels cannot be separated, there is no simple relation between the cross section for the inclusive reaction and the absorptive part of the six-point function. Let us take a particular example: $a=\pi^-$, $b=$ proton, and $c=K^-$. The process which gives the right-hand cut, shown in Fig. 3(a), is nonzero when

$$M^2 \geq (\mu_K + m)^2.$$

(For the left-hand cut see below.) The break in the cut is due to the requirement that $q^2 = \mu_K{}^2$. The cut in the region

$$(\mu_K + m_p)^2 \leq M^2 \leq (\sqrt{s} - \mu_K)^2$$

corresponds to the emission of a K meson, since it can easily be verified that $q_0 \geq \mu_K$. The cut in the region $M^2 \geq (\sqrt{s}+\mu_K)^2$ corresponds to the three-particle scattering process since $q_0 \leq -\mu_K$, provided s and s' are analytically continued to the proper side of the cut.

The left-hand cut comes from the diagram shown in Fig. 3(b). We are interested in the case where s and s' are held fixed and large. In particular, $(p_a - q)^2 = t < 0$, $(p_a - p_b')^2 \approx -s < 0$, $(q+p_b')^2 = s + \mu^2 - M^2 + t$. Then this diagram corresponds to the cross section for the inclusive process $K^- + p \to \pi^- +$ anything and the scattering process $K^- + \pi^+ + p \to$ anything. The incident energies squared for these two reactions are $(p_b + q')^2 = s + \mu^2 - M^2 + t$ and M_1^2, respectively. The square of the momentum transfer between π and K is t. The cut on the M^2 plane corresponding to this process is located at the position

$$M_1^2 = 2t + 2m^2 - M^2 \geq (m_\Sigma + \mu_\pi)^2, \quad M_1^2 = m_\Sigma{}^2.$$

This cut corresponds to the left-hand cut shown in Fig. 4.

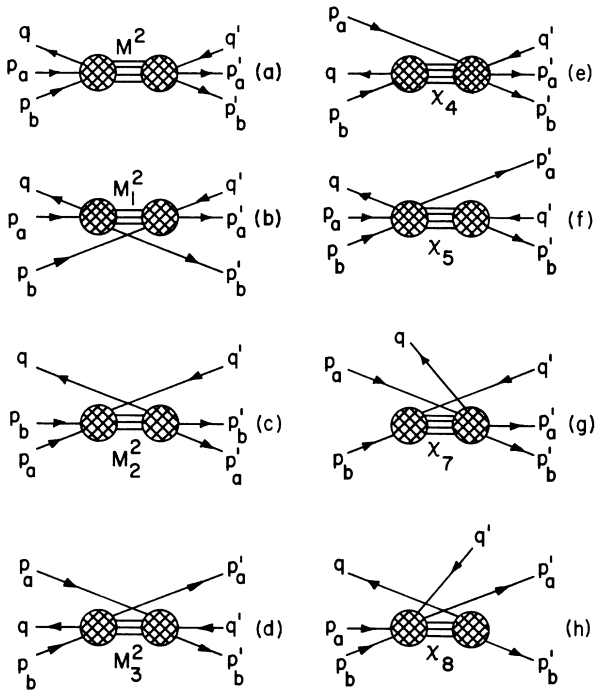

FIG. 3. Channels that have singularities on the M^2 plane when s and t are fixed.

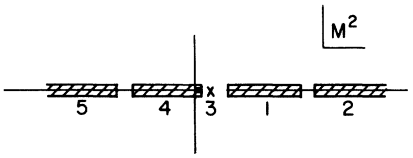

FIG. 4. The singularities of channels M^2 and $M_1{}^2$ on the M^2 plane. The reaction in the M^2 channel is $\pi^- + p \to K^- + X$. The positions of the singularities are: (1) physical region for $\pi^- + p \to K^- + X$, $(m_p + \mu_K)^2 \leq M^2 < (\sqrt{s} - \mu_K{}^2)^2$; (2) region related to $K^+ \pi^- p \to X$, $(\sqrt{s} + \mu_K)^2 \leq M^2$; (3) physical region for $K^- p \to \pi^- + \Sigma^+$, $M^2 = 2t + 2m^2 - m_\Sigma{}^2$; (4) physical region for $K^- p \to \pi^- + X$, $2t + 2m^2 - (\sqrt{s} - \mu)^2 \leq M^2 \leq 2t + 2m^2 - (m_\Sigma + \mu_\pi)^2$; (5) region related to $K^- p \pi^+ \to X$, $M^2 \leq 2t + 2m^2 - (\sqrt{s} + \mu)^2$.

III. COMPLEX CUTS?

So far we have been discussing the singularities whose existence is guaranteed by unitarity. Are there any other singularities? It is our task to investigate the additional singularity structure of the amplitude T, besides the cuts shown in Fig. 4, in the region $|M^2| \leq (\sqrt{s} - \mu_\pi)^2$. We do not have to look far to find such singularities. In fact the box diagram shown in Fig. 5 will give a complex branch point on the physical sheet in the region $|s/M^2| = O(1)$.[6] Another region of interest is where $|s/M^2| \gg 1$. In this region such a trivial example cannot be found. Therefore, restricting oneself to the region $|s/M^2| \gg 1$, we will now investigate the singularity structure implied by a certain class of Feynman diagrams in ϕ^3 theory. We will notice some very important simplifications.

In the region $|s/M^2| \gg 1$, we expect the dominating process in the inclusive reaction to be the Regge exchange shown in Fig. 6. In particular in the case of $\pi^+ p \to \pi^+ + X$ at $M^2 = m_\rho{}^2$, Fig. 6 represents an elastic $\pi^+ p \to \pi^+ p$ process which is dominated by the Pomeranchukon exchange. Experimentally, in the reaction $p + p \to p + X$,[7] it is seen that $I = \frac{1}{2}$ baryon resonances are produced and the cross section is constant in energy. Furthermore, the Δ_{33}-resonance production cross section goes down rapidly with energy. This indicates that in the reaction $pp \to p + X$, Pomeranchukon exchange gives the cross section which is constant in s and the lower-lying trajectories, for example, ρ, give the contribution which decreases with s. In fact

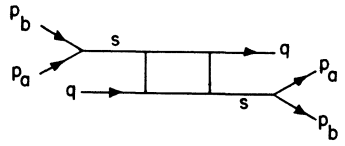

FIG. 5. The box diagram which gives a complex singularity in the physical sheet.

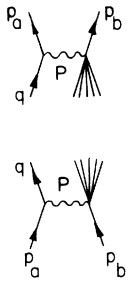

FIG. 6. The dominant diagram in the inclusive reaction at small t and $|s/M^2| \gg 1$.

these experiments tell us that Fig. 6 is the dominant contribution. We use this experimental result to say that in the limit of large $|s/M^2|$, only a certain class of diagrams is important in ϕ^3 theory. Consider the diagram shown in Fig. 7.

(i) The four-point function associated with the lower black blob corresponds to the arbitrary sum of diagrams in ϕ^3 theory, so that it behaves as $[-(p_a + k_1)^2]^{\alpha(t)} \beta(k_1{}^2, (k_1 + p_a - q)^2, t)$ in the limit of large $(p_a + k_1)^2$. Similarly for the upper black blob. Furthermore, we assume that the asymptotic behavior of $\beta(m_1{}^2, m_2{}^2, t)$ on the complex $m_1{}^2$, $m_2{}^2$ plane is such that a double dispersion relation can be written. The ladder diagrams satisfy these criteria.

(ii) The cross-hatched blob is a six-point function which represents an arbitrary Feynman diagram with n propagators and l loops.

From the experimental evidence presented above, in the limit of large s/M^2 the set of diagrams belonging to Fig. 7 gives the dominating contribution to the amplitude. We therefore restrict ourselves to these diagrams. A crucial

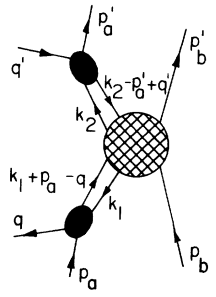

FIG. 7. The class of diagrams in ϕ^3 theory that were studied. It has the following properties: (i) The four-point function associated with the lower black blob corresponds to the arbitrary sum of diagrams in ϕ^3 theory, so that it behaves as $[-(p_a + k_1)^2]^{\alpha(t)} \beta(k_1{}^2, (k_1, + p_a - q)^2, t)$ in the limit of large $(p_a + k_1)^2$. Similarly for the upper black blob. (ii) The cross-hatched blob is a six-point function which represents an arbitrary Feynman diagram with n propagators and l loops.

question is whether the class of diagrams contained in Fig. 7 possesses singularities other than those required by analyticity. To answer this, we will prove in Sec. IV the following theorem.

Theorem. In the limit of large s, the necessary condition for a diagram [Fig. 7 satisfying (i) and (ii) above] to possess complex branch points on the physical M^2 plane is that $\beta(m_1^2, m_2^2, t)$ possesses a complex branch point on the m_1^2 or m_2^2 plane, or a branch point at m_1^2 or $m_2^2 \leq \mu_0^2$. μ_0 is the mass of ϕ.

If $\beta(m_1^2, m_2^2, t)$ possesses only a cut on the real axis at $\mu_0^2 < m_1^2, m_2^2$, the analyticity of the diagram in Fig. 7 can be deduced from that of the diagram in Fig. 8 and only the cut due to unitarity shown in Fig. 3 is present in the amplitude T. This theorem reduces the study of the six-point-function analyticity to that of the four-point Regge-residue function in this particular kinematical limit. For example, if we sum over only the leading logarithm in the ladder diagram, $\beta(m_1^2, m_2^2, t) =$ constant. Thus to this order, Fig. 7 contains cuts only on the real axis corresponding to the unitarity cut shown in Fig. 4. We feel, however, uneasy to restrict ourselves to the leading log since the nonleading log is also important in obtaining the asymptotic behavior of the residue function[8]

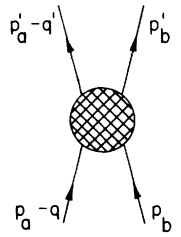

FIG. 8. The diagram whose Feynman denominator function is the same as that of Fig. 7 in the limit of large s.

$$\beta(m_1^2, m_2^2, t) \underset{m_1^2 \to \infty}{\sim} 1/(m_1^2)^{\alpha(t)}. \tag{9}$$

Incidentally, Eq. (9) is consistent with having no complex cut on the m_1^2 plane.

IV. THEOREM

This section contains the proof of the theorem stated above. A reader who is not interested in the details may skip this section without losing continuity. The Feynman amplitude of Fig. 7 with l loops and n propagators in the cross-hatched blob may be written as

$$F \propto \int \prod_{i=1}^{l+2} d^4k_i \frac{\beta(k_1^2, (k_1+p_a-q)^2, t)\beta(k_2^2, (k_2-p_a'+q')^2, t)[-(k_1+p_a)^2]^\alpha [-(k_2-p_a')^2]^\alpha}{(k_1^2-\mu_0^2)[(k_1+p_a-q)^2-\mu_0^2](k_2^2-\mu_0^2)[(k_2-p_a'+q')^2-\mu_0^2]\prod_{r=1}^{n}(q_r^2-\mu_0^2)}, \tag{10}$$

where we have labeled the momenta flowing through the loops by k_i, the momenta associated with the internal lines by q_r, and the mass of the internal particles was taken to be μ_0.[9,10] By the asymptotic behavior assumed in (i) above, we can write an integral representation

$$\begin{aligned}\frac{\beta(k_1^2, (k_1+p_a-q)^2, t)}{(k_1^2-\mu_0^2)[(k_1+p_a-q)^2-\mu_0^2]} &= \int_C \frac{\tilde{\rho}(\mu_1^2, \mu_2^2, t, \mu_0^2)}{(k_1^2-\mu_1^2)[(k_1+p_a-q)^2-\mu_2^2]}\, d\mu_1^2 d\mu_2^2 \\ &+ \int_C \frac{\tilde{\rho}(\mu_0^2, \mu_2^2, t, \mu_0^2)}{(k_1^2-\mu_0^2)[(k_1+p_a-q)^2-\mu_2^2]}\, d\mu_2^2 + \int_C \frac{\tilde{\rho}(\mu_1^2, \mu_0^2, t, \mu_0^2)}{(k_1^2-\mu_1^2)[(k_1+p_a-q)^2-\mu_0^2]}\, d\mu_1^2 \\ &\equiv \int_C \frac{\rho(\mu_1^2, \mu_2^2, t, \mu_0^2)}{(k_1^2-\mu_1^2)[(k_1+p_a-q)^2-\mu_2^2]}\, d\mu_1^2 d\mu_2^2,\end{aligned} \tag{11}$$

where the path of integration μ_1^2, μ_2^2 may be complex depending on the singularity structure of $\beta(m_1^2, m_2^2, t)$. A finite number of subtraction constants will not affect our argument below. Using the representation

$$\frac{(-s)^\alpha}{\sin\pi\alpha} = \frac{1}{\pi}\int \frac{(m^2)^\alpha}{s-m^2+i\epsilon}\, dm^2 \tag{12}$$

which is valid for $\alpha < 0$, we can rewrite Eq. (10):

$$F \propto \int_{\mu_0^2}^{\infty} d\mu_1^2 d\mu_2^2 \rho_1(\mu_1^2, \mu_2^2, t, \mu_0^2)\rho_2(\mu_3^2, \mu_4^2, t, \mu_0^2) \int_0^\infty dm_1^2 dm_2^2 (m_1^2)^\alpha (m_2^2)^\alpha \left(\frac{\sin\pi\alpha}{\pi}\right)^2 G, \tag{13}$$

where

$$G=\int \frac{\prod_{i=1}^{l+2} d^4k_i}{[(k_2+q')^2-m_2^2][k_1^2-\mu_1^2][(k_1+p_a-q)^2-\mu_2^2][k_2^2-\mu_3^2][(k_2-p_a'+q')^2-\mu_4^2][(k_1+p_a)^2-m_1^2]\prod_{r=1}^{n}(q_r^2-\mu_0^2)}$$

$$=(n+5)!\int \prod_{i=1}^{l+2} d^4k_i \prod_{j=1}^{n+6} dx_j \delta\left(1-\sum_{j=1}^{n+6} x_j\right)$$

$$\times\Big\{(k_1^2-\mu_1^2)x_3+[(k_1+p_a-q)^2-\mu_2^2]x_4+(k_2^2-\mu_3^2)x_5+[(k_2-p_a'+q')^2-\mu_4^2]x_6$$

$$+[(k_1+p_a)^2-m_1^2]x_1+[(k_2+q')^2-m_2^2]x_2+\sum_{r=7}^{n+6}(q_r^2-\mu_0^2)x_r\Big\}^{-n-6}. \tag{14}$$

G is the integral involved in the diagram shown in Fig. 9.[11] When the loop integration is performed in Eq. (14), we obtain

$$G\propto\int_0^1 \prod_{j=1}^{n+6} dx_j \frac{\delta(\sum_{j=1}^{n+6}x_j-1)C^{n+4-2l}}{(D+i\epsilon C)^{n+6-2l}}, \tag{15}$$

where C is a function of x only and[12]

$$D=\sum_{k=1}^{6}\tilde{f}_k(x_1,\ldots,x_{n+6})\bar{m}_k^2+\sum_{j=1}^{25}f_j(x_1,\ldots,x_{n+6})\chi_j-\left(\sum_{r=6}^{n+6}x_r\mu_0^2+m_1^2x_1+m_2^2x_2+\mu_1^2x_3+\mu_2^2x_4+\mu_3^2x_5+\mu_4^2x_6\right)C. \tag{16}$$

The χ_j are all possible invariants that can be constructed out of six four-vectors. They are given in footnote 4. The $\bar{m}_k^2$ are external masses. With Eq. (15), the m_1^2, m_2^2 integration in Eq. (13) can be performed explicitly. Note that in order to perform this integration, it is necessary to keep $\alpha<0$, $D'=D+m_1^2x_1+m_2^2x_2\neq 0$. Such a region exists (e.g., where $\bar{m}_k^2\approx 0$, $\chi_j\approx 0$) and analytical continuation to their physical values can be performed after the integration. The result is

$$F\propto\frac{\Gamma^2(\alpha+1)\Gamma(n-2l+4-2\alpha)}{\Gamma(n-2l+6)}\int_{\mu_0^2}^{\infty} d\mu_1^2 d\mu_2^2 I\rho(\mu_1^2,\mu_2^2,t,\mu_0^2)\rho(\mu_3^2,\mu_4^2,t,\mu_0^2), \tag{17}$$

where

$$I=e^{-2\pi i\alpha}\int\prod_{j=1}^{n+6}dx_j\frac{C^{n+2-2l-2\alpha}x_1^{-\alpha-1}x_2^{-\alpha-1}\delta(\sum_{j=1}^{n+6}x_j-1)}{(D')^{n-2l+4-2\alpha}},$$

$$D'=D+m_1^2x_1+m_2^2x_2. \tag{18}$$

In the forward limit and large s, we have

$$s=s'=-s_2=-s_2',\quad t=t',\quad \chi_1=\chi_2=\chi_3=0,$$

$$\chi_4=\chi_5=(p_b-q)^2,\quad \chi_6=\chi_9=-t+2(m^2+q^2), \tag{19}$$

$$\chi_7=\chi_8=(p_b+q')^2,\quad \chi_{10},\ldots,\chi_{15}=\text{masses}^2.$$

Writing D' explicitly,

$$D'=(\tilde{f}_1+\tilde{f}_4+f_{11}+f_{15}+\tilde{f}_2+\tilde{f}_5+f_{10}+f_{12})m^2$$

$$+(\tilde{f}_3+\tilde{f}_6+f_{13}+f_{14})\mu^2+f_4(p_b-q)^2$$

$$+f_5(p_b'-q')^2+(f_6+f_9)[-t+2(m^2+q^2)]+f_7(p_b+q')^2$$

$$+f_8(p_b'+q)^2+(f_{16}-f_{20})s+(f_{17}-f_{21})s'$$

$$+(f_{18}+f_{19})t+f_{22}M^2+f_{23}M_1^2+f_{24}M_2^2+f_{25}M_3^2$$

$$-\left(\sum_{r=6}^{n+6}x_r\mu_0^2+\mu_1^2x_3+\mu_2^2x_4+\mu_3^2x_5+\mu_4^2x_6\right)C. \tag{20}$$

The equality among the invariants in the forward limit is true only for the real part. At this stage it will be seen below that it is important to distinguish s and s'. We can simplify Eq. (20) by the relations (4); the result is

$$D'=g_1M^2+g_2s+g_3s'+g_4t+g_5\mu^2+g_6m^2$$

$$-\left(\sum_{r=6}^{n+6}x_r\mu_0^2+\mu_1^2x_3+\mu_2^2x_4+\mu_3^2x_5+\mu_4^2x_6\right)C, \tag{21}$$

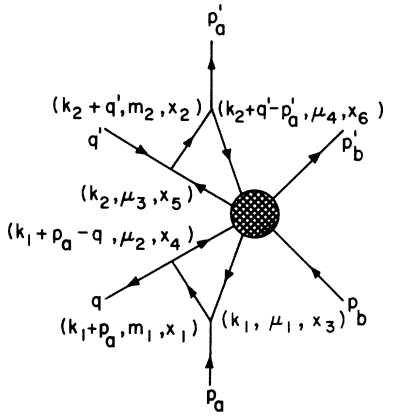

FIG. 9. Diagram for G defined by Eq. (14).

where

$$g_1=(f_4+f_5-f_7-f_8+f_{22}-f_{23}-f_{24}+f_{25}),$$
$$g_2=(-f_4+f_8+f_{16}-f_{20}+f_{24}-f_{25}),$$
$$g_3=(-f_5+f_7+f_{17}-f_{21}+f_{24}-f_{25}),$$
$$g_4=(-f_4-f_5-f_6+f_7+f_8-f_9+f_{18}+f_{19}-2f_{25}),$$
$$g_5=(\tilde{f}_3+\tilde{f}_6+f_4+f_5+f_7+f_8),$$
$$g_6=(\tilde{f}_1+\tilde{f}_2+\tilde{f}_4+\tilde{f}_5+2f_4+2f_5+2f_6+2f_9+f_{10}+f_{11}+f_{12}+f_{15}+2f_{23}+6f_{25}).$$

Equation (17) with the D' function given by Eq. (21) is a general form of the amplitude.

We are interested in a particular kinematical region, namely, large s and s', and s is evaluated on the upper side of the cut in s, s' is evaluated on the lower side of the cut in s', and $t\leq 0$. We cannot simply take the large-s limit of Eq. (17) along the real axis since the integral representation (17) is not defined there. In order to get around this point, we define the functions h_2 and h_3:

$$g_2(x_1,\ldots,x_{n+6})=x_1h_2(x_2,\ldots,x_{n+6}),$$
$$g_3(x_1,\ldots,x_{n+6})=x_2h_3(x_1,x_3,\ldots,x_{n+6}).$$

(We note that $f_j\propto x_1$ for

$$j=1,3,4,6,8,9,10,11,12,13,16,21,24,25$$

and $f_j\propto x_2$ for

$$j=1,3,5,6,7,9,10,12,14,15,17,20,24,25.$$

This follows since we must cut the line associated with x_1 or x_2 to form the invariants χ_j listed in footnote 4.) We divide the integration region of Eq. (15) into four parts by inserting

$$[\theta(h_2)+\theta(-h_2)][\theta(h_3)+\theta(-h_3)]=1 \tag{22}$$

into Eq. (15). Later we will be looking for a term proportional to $s^{2\alpha}$ which comes from the region where $h_1,h_2\gg|1/s|$. Therefore, we can write I as sum of four integrals. (If the integration region where h_2 or $h_3\approx 0$ is important, then it requires extra care.) Calling $I_1,\ldots,I_4$ terms with $\theta(h_2)\theta(h_3)$, $\theta(h_2)\theta(-h_3)$, $\theta(-h_2)\theta(h_3)$, and $\theta(-h_2)\theta(-h_3)$, respectively, we see that I_1 has cuts when $s,s'>0$, I_2 has cuts when $s>0$, $s'<0$, I_3 and I_4 have cuts when $s<0$, $s'>0$ and $s<0$, $s'<0$, respectively. Therefore a large s, s' limit can be taken in the direction where it is regular in s and s', that is $s,s'\to-\infty$ for I_1, $s\to-\infty$, $s'\to\infty$ for I_2, etc. We will demonstrate the technique for I_1. The technique can be applied for $I_2,\ldots,I_4$ also. Writing

$$I_1=e^{-2\pi i\alpha}\int_0^1\prod_{j=1}^{n+6}dx_j\,\delta\Big(\sum_{j=1}^{n+6}x_j-1\Big)\frac{C^{n+2-2l-2\alpha}\theta(h_2)\theta(h_3)x_1^{-\alpha-1}x_2^{-\alpha-1}}{D^{n-2l+4-2\alpha}}\,, \tag{23}$$

we take the large s, s' limit of Eq. (23). Note, however, that Eq. (23) converges only for $\alpha<0$. Therefore, what we must do is to single out the region of integration where I_1 behaves like $s^\alpha s'^\alpha$ and analytically continue to $\alpha<0$ after doing the integration explicitly. Note that for $\alpha<0$, such a term is not the leading term. Furthermore, when $s,s'\to\infty$, the integral representation ceases to be valid since I_1 will diverge when s and s' reach the threshold value for their respective channels. When all other invariants are kept below threshold, in particular negative, the integral is well defined when $s,s'\to-\infty$. I_1 is well defined on the upper-half s and s' planes as well as on the negative real axis, and therefore using the Schwarz reflection principle, it is analytic on the physical sheet of the s and s' planes except for the cut on the real positive axis. Therefore, we can continue the $s,s'\to-\infty$ limit to obtain $s\to\infty+i\epsilon$ and $s'\to\infty-i\epsilon$. (The assumption about the real integration range for $\mu_1,\ldots,\mu_4$ is important here.) Note the presence of $x_1^{-\alpha-1}$, $x_2^{-\alpha-1}$ in the numerator of Eq. (23). When s and s' are large, the integration region $x_1\sim|1/s|$, $x_2\sim|1/s'|$ gives the dominant contribution proportional to $s^\alpha s'^\alpha$. When h_1 or $h_2\sim|1/s|$, the contribution proportional to $s^\alpha s'^\alpha$ does not arise. Therefore, we can restrict ourselves to the region $h_1,h_2\gg|1/s|$. This justifies the splitting of I into $I_1,\ldots,I_4$. First we fix $s'<0$ and take $s\to-\infty$. Setting $y=x_1sh_1/R$,

$$I_1=(-s)^\alpha e^{-i\pi\alpha}\int_0^{sh_1/R}dy\prod_{j=2}^{n+6}dx_j\,\delta\Big(\sum_{j=2}^{n+6}x_j-1\Big)\frac{C^{n+2-2l-2\alpha}\theta(h_2)\theta(h_3)h_1^{\alpha}y^{-\alpha-1}x_2^{-\alpha-1}}{R^{n-2l+4-\alpha}(1+y)^{n-2l+4-2\alpha}}\,, \tag{24}$$

where $R=D-sg_2$. In taking the larger-s limit, the x_1 appearing in R as well as in the δ function and C can be set to zero. I.e., f_j for

$$j=1,3,4,6,8,9,10,11,12,13,21,24,25$$

drops out of the problem. In particular, we note that f_4, f_8, f_{24}, f_{25} corresponding to M_2, M_3, χ_4, χ_8 drop out. So Eq. (24), for large s, does not contain singularities from the channels shown in Figs. 3(c), 3(d), 3(e), 3(h). [Later we will see that when the large-s' limit is taken, the limiting expression does not con-

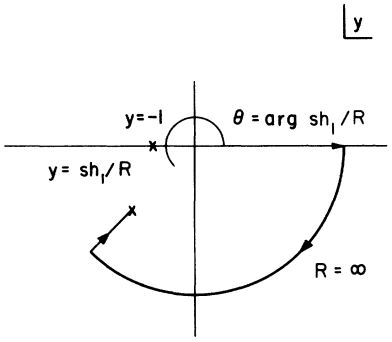

FIG. 10. Path of integration for Eq. (24).

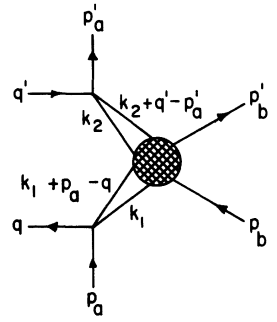

FIG. 11. The diagram which gives the s^{α}, s'^{α} limit when s and s' are large.

tain the singularities from the channels shown in Figs. 3(f) and 3(g) and contains only those in Figs. 3(a) and 3(b).] Note that the path of integration depends on what we take for the phase of sh_1/R. The singularity of the integrand at $y=-1$ never makes the integral diverge. In fact we take the path of integration shown in Fig. 10. Since the value of the integral is zero everywhere except along the positive real axis,

$$I_1 \approx (-s)^{\alpha} e^{-i\pi\alpha} \frac{\Gamma(-\alpha)\Gamma(n-2l+4-\alpha)}{\Gamma(n-2l+4-2\alpha)} \int \prod_{j=2}^{n+6} dx_j \frac{C^{n-2l-2\alpha+2}\theta(h_2)\theta(h_3)h_1{}^{\alpha}x_2{}^{-\alpha-1}}{(R')^{n-2l+4-\alpha}}, \tag{25}$$

$$R' = [R]_{x_1=0}.$$

The large-s' limit can be taken in the same way. Continuing to the region $\alpha>0$, and continuing s and s' from the negative axis to $s_0+i\epsilon$ and $s_0-i\epsilon$, respectively, along the positive real axis, we have

$$I_1 \approx \frac{|s|^{2\alpha}\Gamma^2(-\alpha)\Gamma(n-2l+4)}{\Gamma(n-2l+4-2\alpha)} \int \prod_{j=3}^{n+6} dx_j \frac{C^{n-2l-2\alpha+2}\theta(h_2)\theta(h_3)h_1{}^{\alpha}h_2{}^{\alpha}}{K^{n-2l+4}}, \tag{26}$$

where

$$K = (f_{22}-f_{23})M^2 + (f_{18}+f_{19})t + (\tilde{f}_1+\tilde{f}_2+\tilde{f}_4+\tilde{f}_5+2f_{23})m^2 - \left(\sum_{r=6}^{n+6} x_r\mu_0{}^2 + \mu_1{}^2x_3 + \mu_2{}^2x_4 + \mu_3{}^2x_5 + \mu_4{}^2x_6\right) C. \tag{27}$$

All invariants which were multiplied by x_1 and x_2 were eliminated. Finally,

$$F_1 \propto |s|^{2\alpha} \frac{\Gamma(n+4-2l)}{\Gamma(n-2l+6)} \frac{\pi^2}{\sin^2\pi\alpha} \int_C \prod_{i=1}^{4} d\mu_i \theta(h_2)\theta(h_3)K^{-n+2l-4}\rho_1(\mu_1{}^2, \mu_2{}^2, t, \mu_0{}^2)\rho_2(\mu_3{}^2, \mu_4{}^2, t, \mu_0{}^2)$$

$$\times h_1{}^{\alpha}(x_3, \ldots, x_{n+6})h_2{}^{\alpha}(x_3, \ldots, x_{n+6})C^{n-2l-2\alpha+2}, \tag{28}$$

where the subscript 1 corresponds to the contribution of I_1 to F. Assuming that the μ_i integrations are on the real axis $\mu_i{}^2>\mu_0{}^2$, we can deduce the analyticity of F on the M^2 plane from Eqs. (27) and (28). Note that K is exactly the denominator function for the four-point function when two of the external particles have mass t. Since the region $x_1 \sim 1/s$, $x_2 \sim 1/s'$ gives the contribution, it can be represented by Fig. 11. The four-point function to arbitrary order in the coupling constant has been discussed in many places.[12,13] The only possible additional complication in our problem is that two of the masses are $t<0$, and that some of the internal masses $\mu_1, \ldots, \mu_4$ are integrated from $\mu_0{}^2$ to ∞. But we note that Ref. 13 shows that the propagator is negative definite below threshold when all the external particles are on their mass shell. The continuation from their mass shell to $t<0$ will make the denominator more negative. The same is true for any $\mu_i{}^2>\mu_0{}^2$. Since the integrals over $\mu_i{}^2$ are convergent, we see that F is analytic on the upper-half M^2 plane as well as on $M^2<4\mu_0{}^2$ on the real axis. Then the Schwarz reflection principle can be used to see that F is analytic everywhere on the physical sheet $M^2 \geq 4\mu_0{}^2$ on the real axis. Note that these arguments will be false if $\mu_i{}^2$ is complex, that is, if the residue function $\beta(m_1{}^2, m_2{}^2, t)$ has a singularity on the complex $m_1{}^2$, $m_2{}^2$ plane.

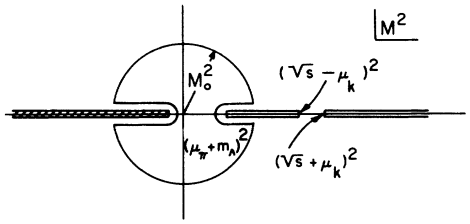

FIG. 12. Analyticity of I on the M^2 plane and the path of integration to obtain the finite-energy sum rule.

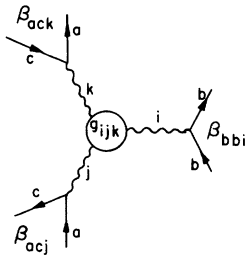

FIG. 13. The triple-Regge diagram.

V. SUM RULE

The theorem states that if there is any complex branch point, the source of such a branch point is in the Regge-residue function of the ordinary two-to-two scattering amplitude. We are not prepared, here, to make any statement about the Regge-residue function. We would rather take the point of view that if the result of assuming no complex branch point on the M^2 plane does not agree with experiment, then we know a possible source of the problem.

In this section, we assume that no other branch point except those coming from unitarity exists. The singularity structure for I is shown in Fig. 12. (For those who skipped Sec. IV, I is the part of T which contains all the leading singularities in the limit of large s.) The discontinuity across the cut, according to Eq. (6), is proportional to the inclusive cross section. Therefore, if we know the M^2 dependence of the amplitude around the circle of radius M_0^2, we can use the formula

$$\oint (M^2)^n I dM^2 = 0 \tag{29}$$

to obtain the relationship between experimentally measurable quantities.[14] The triple-Regge expansion supplies the M^2 dependence around the circular contour. According to the triple-Regge expansion we have

$$T \underset{M^2\to\infty;\, s/M^2\to\infty}{\sim} \frac{\pi}{4m^2} \sum_{ijk}\left[\eta_j\eta_k^*\left(\frac{s}{M^2}\right)^{\alpha_j(t)+\alpha_k(t)} (M^2)^{\alpha_i(0)} \frac{\beta_{bbi}(0)g_{ijk}(t)\xi_i}{\sin\pi[\alpha_i(0)-\alpha_j(t)-\alpha_k(t)]} + \sum_r F_{ijk}^r\right], \tag{30}$$

where

$$\eta_j = \beta_{acj}(t)\frac{e^{-i\pi\alpha_j(t)}\pm 1}{\sin\pi\alpha_j(t)}, \quad \xi_i = e^{-i\pi[\alpha_i(0)-\alpha_j(t)-\alpha_k(t)]}\pm 1.$$

$\beta_{abj}(t)$ is a Regge-residue function associated with particles a and b and the Regge-trajectory j coupling, $g_{ijk}(t)$ is the triple-Regge residue function. They are normalized in the same way as in Ref. 15. These notations are defined by Fig. 13. In particular, our $g_{PPP}(t)$ where P stands for the Pomeranchukon, corresponds to $g_P(t)$ in Ref. 15; $\alpha(0)$ and $\alpha_j(t)$ are the Regge-trajectory functions. When $\alpha_i(0)-\alpha_j(t)-\alpha_k(t) = \gamma =$ integer, the first term of Eq. (30) seems to have spurious poles. They are canceled by either (i) a zero in $g_{ijk}(t)$ or (ii) by F_{ijk}^r. The spurious poles have been studied in Ref. 10 by computing a particular Feynman diagram in ϕ^3 theory. It was found that for $\gamma \leq 0$, $F_{ijk}^n = 0$ and $g_{ijk}(t)$ has a zero; for $\gamma \geq 1$, F_{ijk}^n is present to cancel the poles. It is, therefore, quite reasonable to assume that $F_{ijk}^n = 0$ for $n \leq 0$. For $n \geq 1$, F_{ijk}^n is a polynomial, and even if it is present,

$$\oint F_{ijk}^r (M^2)^n dM^2 = 0$$

and gives no contribution to Eq. (29). Using Eq. (6) and the argument about the left-hand cut presented in Sec. II, we obtain

$$\int_{m^2}^{M_0^2} (M^2)^n \left(\frac{d\sigma}{dtdM^2}\right)_{a+b\to c+X} dM^2 - (-1)^n \int_{m^2}^{M_0^2} (M^2)^n \left(\frac{d\sigma}{dtdM^2}\right)_{c+b\to a+X} dM^2$$

$$= \sum_{ijk}[1-(-1)^n]\frac{\eta_j\eta_k^*}{16\pi s^2}\left(\frac{s}{M_0^2}\right)^{\alpha_j(t)-\alpha_k(t)} (M_0^2)^{\alpha_i(0)+n+1} \frac{\beta_{bbi}(0)g_{ijk}(t)}{\alpha_i(0)-\alpha_j(t)-\alpha_k(t)+n+1}. \tag{31}$$

It is important to point out that for $(d\sigma/dtdM^2)_{c+b\to a+X}$ the invariant energy squared of b and c is

$$(p_b+q)^2 = s+\mu^2-M^2+t$$

and it is not fixed along the integration path. When the major contribution to the integral comes from lower end of the integral, however, the modification due to the energy shift should be small. Note also that if $a=c$, Eq. (31) reduces to a trivial equation for even n.

VI. EXTENSIONS

Equation (31) in general requires measurements of two inclusive cross sections, $a+b\to c+X$ and $c+b\to a+X$. In this section we discuss sum rules which stem from Eq. (31) but require less experimental data. We see immediately that for $a=c$ and odd n we have

$$\int_{m^2}^{M_0^2}(M^2)^n\left(\frac{d\sigma}{dtdM^2}\right)_{a+b\to a+X}dM^2 = \sum_{ijk}\frac{1}{16\pi s^2}\eta_j\eta_k^*\left(\frac{s}{M_0^2}\right)^{\alpha_j(t)+\alpha_k(t)}(M_0^2)^{\alpha_i(t)+n+1}\times\frac{\beta_{bbi}(0)g_{ijk}(t)}{\alpha_i(0)-\alpha_j(t)-\alpha_k(t)+n+1}\,. \tag{32}$$

The contribution from the crossed channel $c+b\to a+X$ in Eq. (31) comes from the fact that I contains both right- and left-hand cuts. Suppose now that we can make the separation $I=I_L+I_R$, where I_R (I_L) is an analytic function of s, t, and M^2 which contains only the right- (left-) hand cut on the M^2 plane in the limit of large s and fixed t. Let us further assume that they both have a triple-Regge behavior with appropriate phase factors (i.e., no fixed poles). A sum rule can be written for both I_L and I_R separately and we obtain, for all n,

$$\int_{m^2}^{M_0^2}(M^2)^n\left(\frac{d\sigma}{dtdM^2}\right)_{a+b\to c+X}dM^2 = \sum_{ijk}\frac{1}{16\pi s^2}\eta_j\eta_k^*\left(\frac{s}{M_0^2}\right)^{\alpha_j(t)+\alpha_k(t)}(M_0^2)^{\alpha_j+n+1}\times\frac{\beta_{bbi}g_{ijk}(t)}{\alpha_i(0)-\alpha_j(t)-\alpha_k(t)+n+1}\,. \tag{33}$$

Let us now discuss the content of this sum rule. (a) Consider a reaction $a+b\to a+X$. Then the leading Regge trajectory is $i=j=k=$Pomeranchuk. For $n=0$, and small t, we can write

$$\int_{m^2}^{M_0^2}\left(\frac{d\sigma}{dtdM^2}\right)_{a+b\to a+X}dM^2 = \frac{1}{16\pi}\,\frac{\beta_{bbP}|\beta_{acP}|^2 g_{PPP}(t)}{1-\alpha_P(0)-2\alpha' t}+\cdots, \tag{34}$$

where α' is the slope of the Pomeranchuk trajectory. If $\alpha_P(0)=1$, $g_{PPP}(t)$ must have a zero at $t=0$. The presence of this zero is well known. (b) Note that the left-hand side of the sum rule (33) contains the integral over the low-missing-mass region and thus it contains the integral over the resonances. We might, therefore, expect the concept of duality from the two-to-two scattering amplitude to appear here in its generalized form. This will be true if the sum rule holds for unusually low M_0^2 with only the leading Regge trajectory in the sum over i. Since the generalized form of duality is widely accepted without any experimental basis, this is a good opportunity to check it. There is also a related question concerning how the Pomeranchukon and the ordinary Regge contributions should be related to the contributions from the resonance and the background. If we take the analogy with the two-particle scattering, we associate the contribution of the background in the M^2 channel with the Pomeranchukon contribution in i, and the contribution of the resonance with the ordinary Regge contribution in i. All these can be checked when the data for various reactions become available. (c) For the time being, we associate the background production with the Pomeranchukon contribution to the right-hand side of Eq. (33). Then we obtain

$$g_{PPP}(t) = \frac{16\pi[1-\alpha_P(0)+2\alpha' t]}{\sigma_a\sqrt{\sigma_b}}\times\int_{m^2}^{M_0^2}dM^2\left[\frac{d\sigma}{dtdM^2}(a+b\to a+X)\right]_{\text{b.g.}}, \tag{35}$$

where the right side is to include only that background contribution which has $s^{2\alpha_P(t)}$ behavior. This equation is useful for obtaining the value for the triple-Pomeranchukon vertex function. Note that Eq. (35) is the most reliable way to obtain $g_{PPP}(t)$. The only other way known at present is to measure the differential cross section in the triple-Regge region. But the cross section is bound to be small due to the zero in $g_{PPP}(t)$ at $t=0$ discussed above, and away from $t=0$ the contribution from cuts may play a role. Another advantage of Eq. (35) is that if the background can be properly separated from the resonance, the knowledge of the low-energy cross section will put a lower bound on $g_{PPP}(t)$.

Furthermore, note that factorization implies that the right-hand side of Eq. (35) is a universal function of t for any a and b. A test of universality

can be made in, for example,

$$p+p\to p+X, \quad \pi^{\pm}+\mathrm{He}\to \mathrm{He}+X,$$
$$\pi^{\pm}+p\to p+X, \quad \pi^{\pm}+p\to \pi^{\pm}+X,$$
$$K^{\pm}+p\to p+X, \quad K^{\pm}+p\to K^{\pm}+X,$$
$$p+\bar{p}\to p+X, \quad \bar{p}+p\to p+X, \text{etc.}$$

The Regge behavior for the unsignatured amplitudes I_R and I_L was assumed in order to obtain the above results. The verification of this assumption is, in itself, extremely interesting. We will illustrate the possibility that the fixed pole may exist by a *heuristic* argument. Consider a (Reggeon + particle) → (Reggeon + particle) scattering where the initial Regge trajectory has spin α_k and the final Regge trajectory has spin α_j. The particle is taken to be spinless. Let the square of the direct-channel energy be M^2. Then at large M^2, the maximum spin-flip amplitude behaves as $(M^2)^{\alpha_i-\alpha_j-\alpha_k}$ where α_i is the Regge trajectory exchanged in the t channel. For example, if $\alpha_j=\alpha_k=1$, the kinematics is same as that of Compton scattering and α_i is a Pomeranchukon. In fact, at $\alpha_i=\alpha_j=\alpha_k=1$, the spin-flip amplitude chooses wrong-signature nonsense. In Compton scattering one needs a fixed pole at this point in order to prevent the Pomeranchukon from decoupling. The triple-Pomeranchukon contribution resembles this possibility. Since the triple Pomeranchukon decouples at $t=0$, it may be an indication that the fixed pole corresponding to the Pomeranchukon in Compton scattering is absent. But it is quite possible that a fixed pole associated with other trajectories may exist.

VII. CONCLUSION

The analyticity of a scattering amplitude has been proven to be a powerful tool in understanding two-to-two reactions. The possibility of using such a tool in the case of three-to-three amplitudes becomes exceedingly complicated. We have demonstrated that in the region $|s/M^2|\gg 1$ there is a good chance that the analyticity of the three-to-three amplitude on the M^2 plane becomes very simple.

Using this analyticity, we have written a sum rule, Eq. (31). This sum rule enables us to evaluate the triple-Regge residue function from low-missing-mass inclusive cross-section data. Such information will be very useful for future experiments at NAL.

The successes of the sum rules written here, when they are compared with experiment, will be quite significant. It means that we can apply the techniques used in two-particle scattering to the analysis of inclusive reactions. If the idea of duality in the generalized form is verified through these sum rules, we should gain confidence in the significance of dual models.

Note added in proof. We have examined $pp\to p+x$ [Ref. 7 and J. V. Allaby *et al.*, CERN Report No. CERN 70-16, 1970 (unpublished)], and $\pi^-+p\to p+x$ [CERN-IHEP collaboration (unpublished)]. The following conclusions were reached: (a) The cross sections are consistent with two-term triple-Regge expansion

$$\frac{d\sigma}{dtdM^2}=\frac{m^2}{(16\pi)^2 s^2}\left[G_{PPf}\left(\frac{s}{M^2}\right)^{2\alpha_P(t)}\left(M^2\right)^{\alpha_f(0)}+G_{ffP}\left(\frac{s}{M^2}\right)^{2\alpha_f(t)}\left(M^2\right)^{\alpha_P(0)}\right].$$

G_{PPf} and G_{ffP} are products of g, β, η; see S. D. Ellis and A. I. Sanda, Phys. Rev. D (to be published). (b) The finite-energy sum rule for inclusive reaction Eq. (32) is indeed satisfied. See S. D. Ellis and A. I. Sanda, NAL Report No. NAL-THY-47 (unpublished).

ACKNOWLEDGMENTS

We would like to thank L. Balazs, S. D. Ellis, D. Gordon, and J. Sullivan for discussions.

---

[1]A. H. Mueller, Phys. Rev. D 2, 2963 (1970).

[2]Reference 1 and also C. E. DeTar *et al.*, Phys. Rev. Letters 26, 675 (1971).

[3]H. P. Stapp, LBL Report No. UCRL-20623, 1971 (unpublished).

[4]For future reference, we list them.

$\chi_1=(p_a-p_a')^2$, $\chi_2=(p_b-p_b')^2$, $\chi_3=(q-q')^2$, $\chi_4=(p_b-q)^2$, $\chi_5=(p_b'-q')^2$, $\chi_6=(p_a+q')^2$, $\chi_7=(p_b+q')^2$, $\chi_8=(p_b'+q)^2$, $\chi_9=(p_a'+q)^2$, $\chi_{10}=(p_a+p_b-p_a')^2$, $\chi_{11}=(p_a+p_b-p_b')^2$, $\chi_{12}=(p_b-q+q')^2$, $\chi_{13}=(p_a+q'-p_a')^2$, $\chi_{14}=(p_b-p_b'+q')^2$, $\chi_{15}=(p_b-p_a'-p_b')^2$, $s=(p_a+p_b)^2\equiv\chi_{16}$, $s'=(p_a'+p_b')^2\equiv\chi_{17}$, $t=(p_a-q)^2\equiv\chi_{18}$, $t'=(p_a'-q')^2\equiv\chi_{19}$, $s_2=(p_b-p_a')^2\equiv\chi_{20}$, $s_2'=(p_b'-p_a)^2\equiv\chi_{21}$, $M^2=(p_a+p_b-q)^2\equiv\chi_{22}$, $M_1^2=(p_a-p_b'-q)^2\equiv\chi_{23}$, $M_2^2=(p_a+p_b-q')^2\equiv\chi_{24}$, $M_3^2=(-p_a'+p_b-q)^2\equiv\chi_{25}$.

[5]This part of the argument is due to Stapp, Ref. 3.

[6]C.-I Tan, Phys. Rev. D 4, 2412 (1971); R. C. Hwa, Phys. Rev. 134, B1086 (1964).

[7]E. W. Anderson *et al.*, Phys. Rev. Letters 16, 855

(1966).
[8]See, for example, G. Tiktopoulos and S. B. Treiman, Phys. Rev. 135, B711 (1964); 136, B1217 (1964).
[9]We have put in the form $\beta[-(k_1+p_a)^2]^\alpha$ as the contribution from the black blob. Later, we will see that the largest contribution comes from the region where $(k_1+p_a)^2$ is large and thus the short cut will be justified.
[10]The method used here is same as that used in S.-J. Chang *et al.*, Phys. Rev. D 4, 3055 (1971).
[11]Taking Eq. (14) and performing the m_1^2, m_2^2 integrations one can show that the term $s^{2\alpha}$ comes from the region of k integration where $(k_1+p_a)^2=(k_2+q')^2\cong s$. Thus the discussion in Ref. 7 is justified.
[12]R. J. Eden, P. Landshoff, D. Olive, and J. Polkinghorne, *The Analytic S-Matrix* (Cambridge Univ. Press, Cambridge, England, 1966).
[13]J. Bjorken and S. Drell, *Relativi' tic Quantum Fields* (McGraw-Hill, New York, 1965).
[14]While this work was in progress, the author has received: M. Einhorn, LBL Report No. UCRL-20688, 1971 (unpublished); P. Olesen, CERN Report No. Th 1376, 1971 (unpublished), both of which recognize the usefulness of the analyticity in M^2 variable.
[15]H. D. I. Abarbanel *et al.*, Phys. Rev. Letters 26, 937 (1971).
[16]Numerical evaluation of these sum rules is in progress [S. D. Ellis and A. I. Sanda (unpublished)].

PHYSICAL REVIEW D VOLUME 6, NUMBER 1 1 JULY 1972

Octet Dominance of Baryon Matrix Elements and the Vanishing of the Neutron Charge Radius

Glennys R. Farrar*
Institute for Advanced Study, Princeton, New Jersey 08540
(Received 13 March 1972)

The baryon form factor g_V of the vector current is investigated. We demonstrate that the d-type contribution to g_V is proportional to the matrix element of a decuplet operator between baryon states. Hence, if a dynamical mechanism exists which suppresses such matrix elements, the neutron charge form factor will be small even for nonzero q^2. This provides an explanation for the observed vanishing of the neutron charge radius.

Quite accurate experimental data have existed for some time on the slope at $q^2=0$ of the charge form factor of the neutron, obtained from scattering thermal neutrons off atomic electrons.[1] It is found to be very close to zero.[2] Elastic electron scattering experiments confirm this result.[3]

In many respects this lack of structure is puzzling. For instance, a perturbation-theoretical calculation with bare nucleons and pions leads to proton and neutron charge radii of the same order of magnitude. It can easily be checked that including the full SU(3) octets of mesons and baryons does not alter this result.

From nonrelativistic considerations, it is apparent why a model of the neutron as "dressed" by a pion cloud will not agree with experiment in this respect. Taking the convention

$$\int d^4x\, e^{iq\cdot x}\langle n|J_\mu^{\text{e.m.}}(x)|n\rangle=\bar{u}(p')\left(F_1(q^2)\gamma_\mu+iF_2(q^2)\frac{\sigma_{\mu\nu}q_\nu}{2M}\right)u(p), \tag{1}$$

one has

$$F_1(q^2)=1-\tfrac{1}{6}q^2\langle r^2\rangle+\cdots,$$

where $\langle r^2\rangle$ is the charge radius, i.e.,

$$\langle r^2\rangle=\int r^2\rho(\vec{r})d^3r\,.$$

Clearly, the vanishing of $\langle r^2\rangle$ can be accomplished by having the charge density, $\rho(\vec{r})$, identically zero. However if the neutron is sometimes a heavy positive particle (proton) and light negative particle (π^-), positive charge would be concentrated at small r so that $\langle r^2\rangle$ would be negative and characterized by the size of the neutron.

We wish to present here another way of viewing the problem which makes it reasonable that the neutron charge form factor should have zero slope. We proceed by considering matrix elements of the octet of vector currents between octet baryon states. The most general form, allowing for nonconservation of the strangeness-changing vector current, is